ELSEVIER

Journal of Photochemistry and Photobiology
A: Chemistry 86 (1995) 219–224

Journal of
PHOTOCHEMISTRY
AND
PHOTOBIOLOGY
A:CHEMISTRY

# Influence of pore size on the intensity of the monomer and excimer-like fluorescence of pyrene adsorbed onto porous glasses

Tsuneo Fujii [a],*, Akira Ishii [a,1], Nobuo Takusagawa [a], Hiromi Yamashita [b], Masakazu Anpo [b],*

[a] *Department of Chemistry and Materials Engineering, Faculty of Engineering, Shinshu University, Wakasato, Nagano 380, Japan*
[b] *Department of Applied Chemistry, College of Engineering, University of Osaka Prefecture, Sakai, Osaka 593, Japan*

Received 20 May 1994; accepted 9 August 1994

## Abstract

The influence of the pore size of calcinated (773 K) porous glasses (average pore diameters, 40, 80 and 300 Å) on the ratio *R* of the emission intensity of the excimer-like fluorescence to that of the monomer fluorescence of pyrene adsorbed on porous glass was examined. *R* decreased with increasing pore size. The results were interpreted on the basis of the photophysical processes of adsorbed pyrene molecules on the surfaces. The ratio of the quantum efficiency for excimer formation from excited dimeric pyrene was estimated to be 1:0.23:0.11 for PG40, PG80 and PG300. The fractal nature of the surfaces of the individual porous glasses played an important role in the photophysical processes of pyrene encapsulated in the pores.

*Keywords:* Fluorescence; Photophysical process; Pyrene; Adsorption; Porous glass; Pore diameter

## 1. Introduction

Photophysical studies of aromatic molecules adsorbed on solid surfaces yield valuable information on the surface properties of the support materials [1–37]. Pyrene is an excellent photophysical probe molecule because it has a long fluorescence lifetime, forms emissive excimers and has a fluorescence spectrum sensitive to the polarity of the environment. Measurement of the steady state and time-resolved fluorescence spectra of pyrene adsorbed on solid surfaces has revealed that some of the adsorbed species form bimolecular ground state associations (BGSAs) from which excimer-like emission occurs on excitation [11,13–15,20,22,24,25,28,31,36,37]. The formation of the excimer-like configuration from the dimeric adsorbed state is very rapid (less than 1 ns), indicating that the geometry, which emits the excimer-like fluorescence, originates from the conformation of the BGSAs. The effect of pore size on the fluorescence spectrum of adsorbed pyrene on solid surfaces is also an interesting problem [30–35].

In previous papers, we have reported the fluorescence, fluorescence excitation and time-resolved fluorescence spectra of pyrene adsorbed on calcinated (773 K) Vycor glass (average pore diameter, 40 Å) [36]. The influence of the evacuation temperature after the adsorption procedure on the fluorescence spectrum was noted [37]. This paper investigates the influence of the pore size on the fluorescence character of adsorbed pyrene and the ratio *R* of the emission intensity of the excimer-like fluorescence to that of the monomeric fluorescence of pyrene adsorbed onto three porous glasses (diameters, 40, 80 and 300 Å; hereafter abbreviated as PG40, PG80 and PG300 respectively). It is concluded that the pore size of the porous glass plays an important role in the photophysical processes of adsorbed pyrene molecules at the solid surfaces.

## 2. Experimental details

### 2.1. Materials

Pyrene (supplied by Wako Co.) was purified by repeated recrystallization from ethanol and by 230 passes through a zone refiner. Cyclohexane (supplied by Wako Co., Luminasol grade) was used without further puri-

---

* Corresponding authors.

[1] Present address: Nichicon Corporation, Nagano Factory, Toyoshina, Minamiazumi, Nagano 399-82, Japan.

1010-6030/95/$09.50
*SSDI* 1010-6030(94)03947-X

fication. Three different porous glasses (PGs) were used: PG40 is porous Vycor glass (Corning, Code No. 7930; average pore diameter, 40 Å; Brunauer–Emmett–Teller (BET) surface area, 155 $m^2 g^{-1}$); PG80 (average pore diameter, 80 Å; BET surface area, about 100 $m^2 g^{-1}$) and PG300 (average pore diameter, 300 Å; BET surface area, about 50 $m^2 g^{-1}$) were prepared in accordance with the literature [38]. The pore size (width) distribution and BET surface areas for the three PGs were evaluated from the nitrogen adsorption–desorption isotherm using a Carlo Erba Sorptomatic or ASAP 2000 automatic surface area analyser.

### 2.2. Adsorption procedure

Since the detailed adsorption procedure and determination of the extent of adsorption of pyrene on porous glass have been described previously [37], only an outline of the procedure is presented here. Prior to the experiments, a sheet of porous glass (1 mm×5 mm×20 mm) was heat at 773 K for more than 6 h in air to remove all carbonaceous impurities. The sheet was transferred to a quartz cell and degassed in vacuo (less than $1\times10^{-5}$ Torr) at 773 K for 5 h and cooled to 295 K. The adsorption of pyrene molecules onto the porous glass was carried out by pouring a degassed cyclohexane solution of pyrene into the quartz cell in which the preheated porous glass had been placed in vacuo at 295 K. The cyclohexane solutions were subjected to five or six freeze–pump–thaw cycles to remove oxygen before the adsorption procedure. After impregnation for over 5 h, the supernatant solution was removed by decantation and then evacuated in vacuo for 5 h at 373 K (because 373 K is higher than the boiling point of cyclohexane (353 K), a "dry" surface was generated). The quartz cells were sealed under vacuum, and these samples were used for the measurements.

The amount of pyrene adsorbed on the porous glass was determined by measuring the difference between the absorption spectra of the original and supernatant solutions [37]. The surface coverage of pyrene in the experiments was determined from the amount of pyrene adsorbed on the porous glass assuming that an adsorbed pyrene molecule occupies a surface area of 100 $Å^2$ [20]. The amount of pyrene adsorbed on the porous glass ($C$), $C^{1/2}$ and the corresponding surface coverage for PG40, PG80 and PG300 are given in Table 1.

### 2.3. Spectral measurement

The absorption and fluorescence spectra were recorded using a Hitachi 220 recording spectrometer and a Hitachi F-300 fluorescence spectrometer respectively. The quartz cells containing the porous glass for emission measurements were aligned at an angle of 30° to avoid reflection of the exciting light into the slit of the monochromator. The data were transferred to an NEC PC-9801 microcomputer for processing.

Table 1
Amount of adsorbed pyrene on the porous glasses, square root of the amount of adsorbed pyrene and the corresponding surface coverage

| Amount of adsorbed pyrene $C$ ($10^6$ mol $g^{-1}$) | $C^{1/2}$ | Surface coverage |
|---|---|---|
| PG40 | | |
| 0.17 | 0.41 | 0.00065 |
| 0.56 | 0.75 | 0.0022 |
| 5.2 | 2.3 | 0.020 |
| 28 | 5.3 | 0.11 |
| 30 | 5.5 | 0.12 |
| PG80 | | |
| 0.16 | 0.40 | 0.00098 |
| 1.5 | 1.2 | 0.0091 |
| 11 | 3.4 | 0.069 |
| PG300 | | |
| 0.10 | 0.32 | 0.0013 |
| 1.2 | 1.1 | 0.015 |
| 8.2 | 2.9 | 0.099 |
| 19 | 4.4 | 0.23 |

Correction is needed to compare the fluorescence intensity of the pyrene monomer with that of the excimer-like intensity in the three glasses. The relative intensity of the pyrene monomer fluorescence at 470 nm to that at 393 nm in dilute ethanol or glycerol solutions is about 100:3. Therefore a value of 3.0 was subtracted from the intensity of adsorbed pyrene at 470 nm to obtain individual $R$ values.

## 3. Results and discussion

### 3.1. Influence of pore size on the fluorescence spectra

Figs. 1, 2 and 3 show the dependence of the fluorescence spectrum of pyrene on the amount of pyrene molecules adsorbed on PG40, PG80 and PG300 respectively. The excitation wavelength of 372 nm corresponds to the $^1L_b$ transition of pyrene. It can be seen that the entire fluorescence spectrum is composed of the monomer-like emission ($F_M$), exhibiting a sharp vibrational fine structure at around 380–430 nm, and the excimer-like emission ($F_E$), exhibiting a broad band at around 440–550 nm. The ratio $R$ of the intensity of $F_M$ to $F_E$ increases in the order PG40 > PG80 > PG300. $R$ also increases with increasing amount of adsorbed pyrene.

Fig. 4 shows the fluorescence spectrum of pyrene adsorbed on PG40 excited at 334 nm, which corresponds to the $^1L_a$ transition region of pyrene. The characteristic

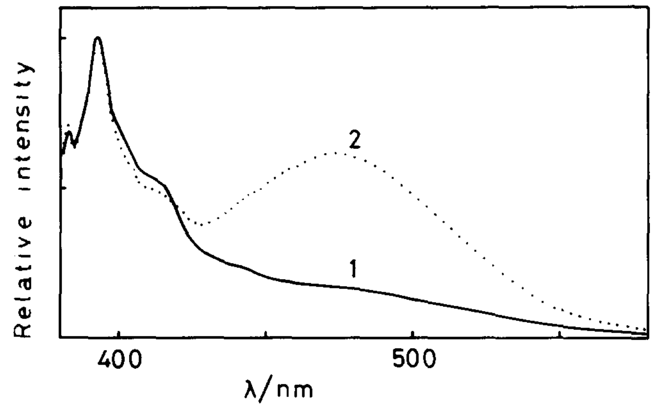

Fig. 1. Dependence of the fluorescence spectrum on the amount of adsorbed pyrene on PG40. Amount of adsorbed pyrene: 1, $1.7\times10^{-7}$ mol $g^{-1}$; 2, $2.8\times10^{-5}$ mol $g^{-1}$. Excitation wavelength, 372 nm.

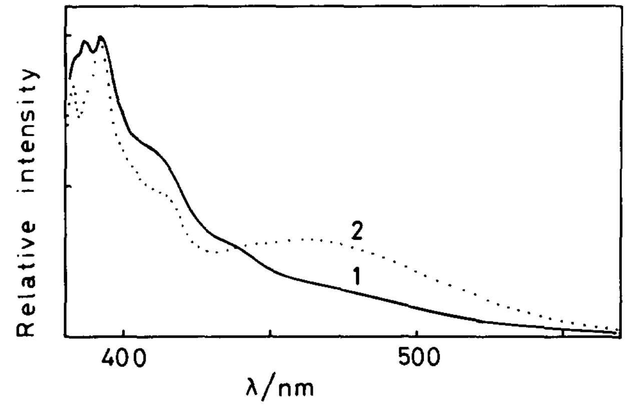

Fig. 2. Dependence of the fluorescence spectrum on the amount of adsorbed pyrene on PG80. Amount of adsorbed pyrene: 1, $1.6\times10^{-7}$ mol $g^{-1}$; 2, $1.1\times10^{-5}$ mol $g^{-1}$. Excitation wavelength, 372 nm.

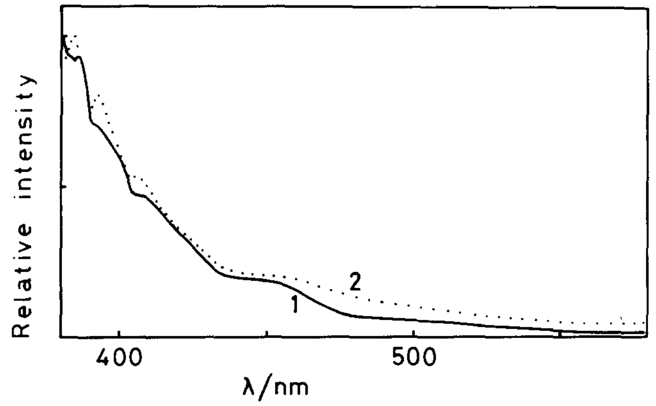

Fig. 3. Dependence of the fluorescence spectrum on the amount of adsorbed pyrene on PG300. Amount of adsorbed pyrene: 1, $1.0\times10^{-7}$ mol $g^{-1}$; 2, $1.9\times10^{-5}$ mol $g^{-1}$. Excitation wavelength, 372 nm.

fine structure of the fluorescence spectrum for monomeric pyrene is evident. No significant difference is observed between the fluorescence spectra for different amounts of adsorbed pyrene. Similar fluorescence behaviour was also observed for PG80 and PG300. The 372 nm band (the 0–0 band) has a relatively high intensity compared with that in polar solvents [39–41].

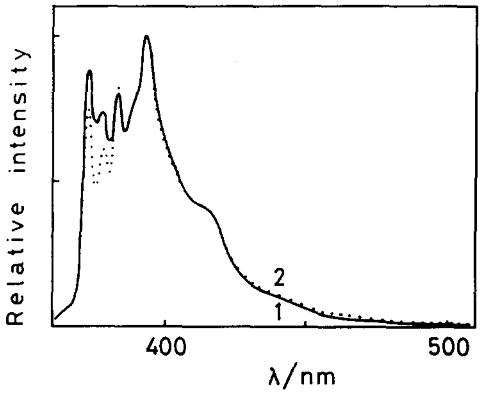

Fig. 4. Dependence of the fluorescence spectrum on the amount of adsorbed pyrene on PG40. Amount of adsorbed pyrene: 1, $1.7\times10^{-7}$ mol $g^{-1}$; 2, $2.8\times10^{-5}$ mol $g^{-1}$. Excitation wavelength, 334 nm.

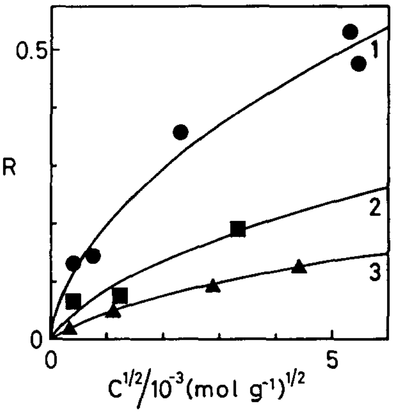

Fig. 5. Relationship between $R$ and $C^{1/2}$: (1) PG40 (●); (2) PG80 (■); (3) PG300 (▲). Full lines are the result of the least-squares method.

The results indicate that the adsorbed pyrene molecules on the surfaces are surrounded by a relatively polar environment. The dependence of the fluorescence spectrum of pyrene on the excitation wavelength indicates that there are more than two ground state species of pyrene; one is the monomeric form and the other is the BGSA which leads to excimer-like emission due to geometrical relaxation of its excited state [11,13,22,24,25,36,37].

### *3.2. Influence of pore size on the photophysical processes*

Fig. 5 shows the relationship between $R$ and the square root of the amount of adsorbed pyrene $C^{1/2}$ ((moles per gram of porous glass)$^{1/2}$) for the three porous glasses. The $R$ values are dependent on the amount of adsorbed pyrene and on the diameter of the porous glass.

Based on the proposed photophysical processes of adsorbed pyrene molecules on the dry surface of silica gel pores (Fig. 6) [25,37], $R$ can be represented as

$$R=a[(1+8KC)^{1/2}-1] \quad (1)$$

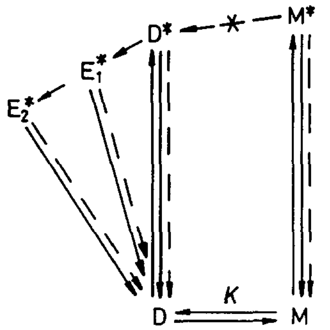

Fig. 6. Dynamics of photophysical processes of pyrene adsorbed onto porous glass. M and D indicate monomeric and dimeric pyrene. M* and D* are excited monomeric and dimeric pyrene (excited directly from M and D). $K$ denotes an equilibrium constant between ground state monomeric and dimeric pyrene. $E_1$* and $E_2$* represent two excimers of pyrene with different configurations on the surface. They are generated from the geometrical relaxation of D*.

Table 2
Results of the least-squares calculations for PG40, PG80 and PG300. $a$ is defined by Eq. (2) and $K$ is the equilibrium constant in Eq. (1). $\sqrt{\Delta r^2}$ and $r_i$ are the $r$-squared and correlation coefficients

| Glass | $a$ | $K$ | $\sqrt{\Delta r^2}$ | $r_i$ |
|---|---|---|---|---|
| PG40 | 0.0396 | 4.43 | $2.54\times10^{-2}$ | 0.988 |
| PG80 | 0.0498 | 0.802 | $1.87\times10^{-2}$ | 0.949 |
| PG300 | 0.0351 | 0.549 | $3.37\times10^{-4}$ | 0.999 |

where $K$ denotes an equilibrium constant between ground state monomeric pyrene and dimeric pyrene on the solid surface and is dependent on the preheating temperature, adsorption procedure and diameter of the porous glass, and $a$ is defined as

$$a=\frac{\epsilon_D\phi_{ED}\phi_E}{4K\epsilon_M\phi_M} \tag{2}$$

where $\epsilon_M$ and $\epsilon_D$ are the absorption coefficients for monomeric and dimeric pyrene respectively at the excitation wavelength, $\phi_E$ and $\phi_M$ are the fluorescence quantum efficiencies for the emissions $F_E$ and $F_M$ respectively and $\phi_{ED}$ is the quantum efficiency of excimer formation from the excited dimeric unit (D*). It should be noted that, at a sufficiently high concentration of adsorbed pyrene molecules, Eq. (1) indicates that $R \alpha C^{1/2}$ if $8KC \gg 1$.

It can be seen from Fig. 5 that the experimental results for the three porous glasses are well reproduced by Eq. (1). Results of least-squares calculations for PG40, PG80 and PG300 are given in Table 2. The differences in $a$ and $K$ are responsible for the differences in the curves for the three porous glasses.

Since the spectral features of the emission $F_M$ and $F_E$ of adsorbed pyrene molecules are similar for the three porous glasses, $\epsilon_M$, $\phi_M$, $\epsilon_D$ and $\phi_E$ in Eq. (2) may be unchanged or not substantially changed for the three glasses. The origin of the difference in the curves is therefore attributable to the difference in the values of $\phi_{ED}$ and $K$. Reciprocal values of $K$ for PG40, PG80 and PG300 are 0.226, 1.25 and 1.82 (1.00:5.53:8.05) respectively. On the other hand, the $a$ values decrease as 0.0659, 0.0498 and 0.0351 (1.00:0.756:0.533). Therefore it is impossible to explain the difference in the $a$ values by the difference in $K$, although the $K$ value for PG40 is extremely large. The difference in the $a$ values reflects other surface properties experienced by the pyrene molecules on PG40, PG80 and PG300. The difference between the curves in Fig. 5 must therefore also be attributed to the difference in $\phi_{ED}$, the quantum efficiency of excimer formation from excited dimeric pyrene. $\phi_{ED}$ can be written as

$$\phi_{ED}=a\times K\times\text{constant} \tag{3}$$

The $\phi_{ED}$ ratio can be estimated as 1.0:0.23:0.11 for PG40, PG80 and PG300 respectively. $\phi_{ED}$ in solution depends on the diffusion between one excited pyrene molecule and one ground state pyrene molecule. However, the process of excimer-like formation on solid surfaces should be very fast [11,36] and not diffusion controlled. The difference between the samples can be attributed to the difference in the geometrical factor due to the different diameters of PG40, PG80 and PG300.

Fig. 7 illustrates a probable configuration of pyrene molecules adsorbed into the pores of PG40, PG80 and PG300. Because the diameter of PG40 is small, the neighbouring pyrene molecules are not aligned in the same plane and tend to have a face-to-face configuration. On the other hand, the diameter of PG300 is relatively large and hence the neighbouring pyrene molecules can be aligned in the same plane. The configuration in the pores of PG80 is intermediate between PG40 and PG300. It is well known that two molecules forming an excimer are arranged in parallel or near-parallel pairs [42]. Therefore we can conclude that excimer formation from excited dimeric pyrene adsorbed in the pores of a porous glass with a small diameter is easier than that adsorbed in a porous glass with a large diameter.

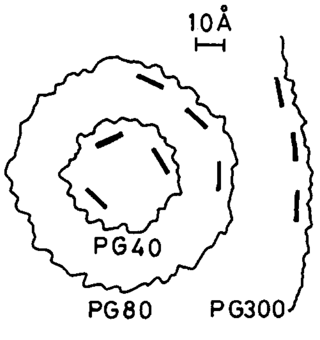

Fig. 7. Illustration of the configuration of pyrene molecules adsorbed into the pores of PG40, PG80 and PG300.

## 4. Conclusions

The emission $F_E$ of pyrene molecules adsorbed on "dry" surfaces originates from "static" dimeric pyrenes formed in the ground state. To form an excimer-like geometry, after excitation of dimeric pyrene, relaxation to a more favourable configuration is required. Association is affected by the heterogeneity of the adsorption sites. In narrow diameter silica gel, a substantial fraction of dimeric pyrenes in the ground state generate an excimer-like conformation on excitation via a dynamic process between neighbouring units involving intramolecular rearrangement. In this case, the face-to-face conformation of dimeric pyrenes is effective for the attractive forces between pyrene units. Therefore the fractal nature of the solid surface [32–35] of the glasses may reflect this tendency and play an important role in the generation of the excimer-like configuration. The excimer-forming order of the solid surfaces agrees with the estimated surface fractal dimensions for PG40, PG80 and PG300 of approximately 2.9, 2.7 and 2.4 respectively [32].

## Acknowledgments

The authors wish to thank the referee for valuable suggestions. They also wish to thank Dr. T. Kawaguchi (ASAHI Glass Co. Ltd.) for measurement of the pore size distribution curves and surface areas of PG80 and PG300. This work was supported in part by a Grant-in-Aid on Priority-Area-Research "Photoreaction Dynamics" from the Ministry of Education, Science and Culture of Japan (No. 06239105).

## References

[1] M. Anpo and T. Matsuura (eds.), *Photochemistry on Solid Surface,* Elsevier, Amsterdam, 1989, and references cited therein.

[2] C.H. Nicholls and P.A. Leemakers, *Adv. Photochem., 8* (1971) 3125.

[3] D. Oelkrug, W. Flemming, R. Fillemann, R. Gunther, W. Honnen, G. Krabichler, M. Schafer and S. Uhl, *Pure Appl. Chem., 86* (1986) 1207, and references cited therein.

[4] P. de Mayo and L.J. Johnston, *Preparative Chemistry Using Supported Reagents,* Academic Press, New York, 1987, p. 61, and references cited therein.

[5] M. Anpo, H. Nishiguchi and T. Fujii, *Res. Chem. Intermed., 13* (1990) 73.

[6] S.L. Suib, in F. Rabek (ed.), *Photochemistry and Photophysics,* Vol. 3, CRC Press, Boca Raton, FL, 1991.

[7] H.P. Leftin, *J. Phys. Chem., 64* (1960) 1714.

[8] H. Ishida and H. Tsubomura, *J. Photochem., 2* (1973) 285.

[9] D. Oelkrug, M. Radjaipour and H. Erbse, *Z. Phys. Chem., Neue Folge, 88* (1974) 23; M. Plaushinat, G. Krabichler, S. Uhl and D. Oelkrug, *J. Mol. Struct., 115* (1984) 351.

[10] P.L. Piciulo and J.W. Sutherland, *J. Am. Chem. Soc., 101* (1979) 3123.

[11] K. Hara, P. de Mayo, W.R. Ware, A.C. Weedon, G.S.K. Wong and K.C. Wu, *Chem. Phys. Lett., 69* (1980) 105.

[12] R.K. Kesseler and F. Wilkinson, *J. Chem. Soc., Faraday Trans. 1, 77* (1981) 309; F. Wilkinson, *J. Chem. Soc., Faraday Trans. 2, 82* (1986) 2077.

[13] R.K. Bauer, R. Borenstein, P. de Mayo, K. Okada, M. Rafalska, W.R. Ware and K.C. Wu, *J. Am. Chem. Soc., 104* (1982) 4635; R.K. Bauer, P. de Mayo, W.R. Ware and K.C. Wu, *J. Phys. Chem., 86* (1982) 3781; R.K. Bauer, P. de Mayo, W.R. Ware and K.C. Wu, *J. Phys. Chem., 87* (1983) 460; R.K. Bauer, P. de Mayo, L.V. Natarajan and W.R. Ware, *Can. J. Chem., 62* (1984) 1279.

[14] P. de Mayo, L.V. Natarajan and W.R. Ware, *J. Phys. Chem., 89* (1985) 3526; P. de Mayo. L.V. Natarajan and W.R. Ware, *J. Phys. Chem., 89* (1985) 3576.

[15] C. Francis, J. Lin and L.A. Thomas, *Chem. Phys. Lett., 94* (1983) 162.

[16] N. Nakashima and D. Phillips, *Chem. Phys. Lett., 97* (1983) 337.

[17] K. Kemnitz, N. Tamai, I. Yamazaki, N. Nakashima and K. Yoshihara, *J. Phys. Chem., 91* (1987) 1423.

[18] C.H. Lochmüller, A.C. Colborn, M.L. Hunnicutt and J.M. Harris, *J. Am. Chem. Soc., 106* (1984) 4077.

[19] N.J. Turro, C.C. Cheng and W. Mahler, *J. Am. Chem. Soc., 106* (1984) 7705.

[20] S.L. Suib and A. Kostapapas, *J. Am. Chem. Soc., 106* (1984) 7705.

[21] G. Beck and J.K. Thomas, *Chem. Phys. Lett., 94* (1983) 553.

[22] D. Avnir, R. Busse, M. Ottolenghi, E. Weller and K. Zachariasse, *J. Phys. Chem., 89* (1985) 3521; E. Weller, D. Rojanski, M. Ottolenghi, D. Huppert and D. Avnir, *J. Am. Chem. Soc., 109* (1987) 575.

[23] C.T. Lin and W.L. Hsu, *J. Lumin., 38* (1987) 305; C.T. Lin, W.L. Hsu, C.L. Yang and M.A. El-Sayed, *J. Phys. Chem., 91* (1987) 4556; C.T. Lin, W.L. Hsu and C.L. Yang, *J. Phys. Chem., 92* (1988) 1889; C.T. Lin and W.L. Hsu, *J. Lumin., 40/41* (1988) 743.

[24] T. Fujii, *Chem. Express, 1* (1986) 331; T. Fujii and E. Shimizu, *Chem. Phys. Lett., 137* (1987) 448.

[25] T. Fujii, E. Shimizu and S. Suzuki, *J. Chem. Soc., Faraday Trans. 1, 84* (1988) 4387.

[26] J. Stahlberg, M. Almgren and J. Alsins, *Anal. Chem., 60* (1988) 2487.

[27] X. Liu, K.-K. Iu and J.K. Thomas, *J. Phys. Chem., 93* (1989) 4120.

[28] H. Lochmüller and T.J. Wenzel, *J. Phys. Chem., 94* (1990) 4230.

[29] T. Suga and T. Hikida, *J. Photochem. Photobiol. A: Chem., 63* (1992) 91.

[30] J.M. Drake and J. Klafter, *J. Lumin., 31/32* (1984) 642.

[31] E. Weller, M. Ottolenghi, D. Avnir and D. Huppert, *Langmuir, 2* (1986) 616.

[32] D. Pines-Rojanski, D. Huppert and D. Avnir, *Chem. Phys. Lett., 139* (1987) 109.

[33] J. Samuel, M. Ottolenghi and S. Avnir, *J. Phys. Chem., 95* (1991) 1890.

[34] D. Pines and D. Huppert, *Israel J. Chem., 29* (1989) 473.

[35] T. Wolff, F. Akbarian and G. von Bünau, *Ber. Bunsenges. Phys. Chem., 94* (1990) 883.

[36] T. Fujii, A. Ishii, S. Suzuki and M. Anpo, *Chem. Express, 4* (1989) 471; T. Fujii, A. Ishii, H. Satozono, S. Suzuki, M. Che and M. Anpo, *Bull. Chem. Soc. Jpn., 63* (1990) 2475.

[37] T. Fujii, A. Ishii, H. Satozono, S. Suzuki, N. Takusagawa and M. Anpo, *J. Photochem. Photobiol. A: Chem.*, accepted for publication.

[38] N. Takusagawa, K. Yanagida and K. Kitajima, *J. Non-Cryst. Solids, 95* (1987) 1055.

[39] A. Nakajima, *Bull. Chem. Soc. Jpn., 44* (1971) 3272.

[40] K. Kalyanasundaram and J.K. Thomas, *J. Am. Chem. Soc., 99* (1977) 2039.

[41] P. Lianos and S. Georghiou, *Photochem. Photobiol., 30* (1979) 355.

[42] J.B. Birks, *Photophysics of Aromatic Molecules,* Wiley-Interscience, London, 1970.